Mechanistic Control of Product Selectivity. Reactions between *cis*-/*trans*-$[Os^{VI}(tpy)(Cl)_2(N)]^+$ and Triphenylphosphine Sulfide

My Hang V. Huynh, Peter S. White, and Thomas J. Meyer*,†

Venable and Kenan Laboratories, Department of Chemistry, The University of North Carolina at Chapel Hill, Chapel Hill, North Carolina 27599-3290

Received December 14, 1999

Reactions between the Os(VI)−nitrido complexes *cis*- and *trans*-$[Os^{VI}(tpy)(Cl)_2(N)]^+$ (tpy is 2,2′:6′,2″-terpyridine) and triphenylphosphine sulfide, $SPPh_3$, give the corresponding Os(IV)−phosphoraniminato, $[Os^{IV}(tpy)(Cl)_2(NPPh_3)]^+$, and Os(II)−thionitrosyl, $[Os^{II}(tpy)(Cl)_2(NS)]^+$, complexes as products. The Os−N bond length and Os−N−P angle in *cis*-$[Os^{IV}(tpy)(Cl)_2(NPPh_3)](PF_6)$ are 2.077(6) Å and 138.4(4)°. The rate law for formation of *cis*- and *trans*-$[Os^{IV}(tpy)(Cl)_2(NPPh_3)]^+$ is first order in both $[Os^{VI}(tpy)(Cl)_2(N)]^+$ and $SPPh_3$ with k_{trans}(25 °C, CH_3CN) = 24.6 ± 0.6 M^{-1} s^{-1} and k_{cis}(25 °C, CH_3CN) = 0.84 ± 0.09 M^{-1} s^{-1}. As found earlier for $[Os^{II}(tpm)(Cl)_2(NS)]^+$, both *cis*- and *trans*-$[Os^{II}(tpy)(Cl)_2(NS)]^+$ react with PPh_3 to give $[Os^{IV}(tpy)(Cl)_2(NPPh_3)]^+$ and $SPPh_3$. For both complexes, the reaction is first order in each reagent with k_{trans}(25 °C, CH_3CN) = (6.79 ± 0.08) × 10^2 M^{-1} s^{-1} and k_{cis}(25 °C, CH_3CN) = (2.30 ± 0.07) × 10^2 M^{-1} s^{-1}. The fact that both reactions occur rules out mechanisms involving S atom transfer. These results can be explained by invoking a common intermediate, $[Os^{IV}(tpy)(Cl)_2(NSPPh_3)]^+$, which undergoes further reaction with PPh_3 to give $[Os^{IV}(tpy)(Cl)_2(NPPh_3)]^+$ and $SPPh_3$ or with $[Os^{VI}(tpy)(Cl)_2(N)]^+$ to give $[Os^{IV}(tpy)(Cl)_2(NPPh_3)]^+$ and $[Os^{II}(tpy)(Cl)_2(NS)]^+$.

Introduction

In an earlier paper, we described a reaction between $[Os^{II}(tpm)(Cl)_2(NS)]^+$ (tpm = tris(pyrazol-1-yl)methane) and PPh_3 which gives as products $[Os^{IV}(tpm)(Cl)_2(NPPh_3)]^+$ and $SPPh_3$, eq 1.[1] The reaction is first order in both

$$[Os^{II}(tpm)(Cl)_2(NS)]^+ + 2PPh_3 \rightarrow [Os^{IV}(tpm)(Cl)_2(NPPh_3)]^+ + SPPh_3 \quad (1)$$

$[Os^{II}(tpm)(Cl)_2(NS)]^+$ and PPh_3 with k(25 °C, CH_3CN) = 40 ± 1 M^{-1} s^{-1}. One mechanism that was proposed was S atom transfer

$$[Os^{II}(tpm)(Cl)_2(NS)]^+ PPh_3 \rightarrow [Os^{VI}(tpm)(Cl)_2(N)]^+ + SPPh_3 \quad (2a)$$

followed by reaction between the released nitrido complex and PPh_3 which is known to be rapid[2]

$$[Os^{VI}(tpm)(Cl)_2(N)]^+ + PPh_3 \rightarrow [Os^{IV}(tpm)(Cl)_2(NPPh_3)]^+ \quad (2b)$$

A second mechanism proposed formation of an intermediate

$$[Os^{II}(tpm)(Cl)_2(NS)]^+ + PPh_3 \rightarrow [Os^{IV}(tpm)(Cl)_2(NSPPh_3)]^+ \quad (3a)$$

followed by rapid reaction with PPh_3

$$[Os^{IV}(tpm)(Cl)_2(NSPPh_3)]^+ + PPh_3 \rightarrow [Os^{IV}(tpm)(Cl)_2(NPPh_3)]^+ + SPPh_3 \quad (3b)$$

We have subsequently discovered that both *cis*- and *trans*-$[Os^{VI}(tpy)(Cl)_2(N)]^+$ (tpy is 2,2′:6′,2″-terpyridine) undergo reactions with $SPPh_3$ to give the corresponding cis and trans isomers of $[Os^{II}(tpy)(Cl)_2(NS)]^+$ and $[Os^{IV}(tpy)(Cl)_2(NPPh_3)]^+$, eq 4. Both of the thionitrosyl complexes also undergo reactions

$$2[Os^{VI}(tpy)(Cl)_2(N)]^+ + SPPh_3 \rightarrow [Os^{II}(tpy)(Cl)_2(NS)]^+ + [Os^{IV}(tpy)(Cl)_2(NPPh_3)]^+ \quad (4)$$

with PPh_3 to give $SPPh_3$ as in eq 1. We show here that the fact that both reactions occur rules out mechanisms involving simple S atom transfer. The results can be explained by invoking a common intermediate that undergoes subsequent reactions with either $[Os^{VI}(tpy)(Cl)_2(N)]^+$ or PPh_3.

The following abbreviations are used in this study: *trans*-$[Os^{VI}{\equiv}N]^+$, *trans*-$[Os^{VI}(tpy)(Cl)_2(N)]^+$, *trans*-$[Os^{II}{-}NS]^+$, *trans*-$[Os^{II}(tpy)(Cl)_2(NS)]^+$, *trans*-$[Os^{IV}{-}NPPh_3]^+$, *trans*-$[Os^{IV}(tpy)(Cl)_2(NPPh_3)]^+$, *cis*-$[Os^{VI}{\equiv}N]^+$, *cis*-$[Os^{VI}(tpy)(Cl)_2(N)]^+$, *cis*-$[Os^{II}{-}NS]^+$, *cis*-$[Os^{II}(tpy)(Cl)_2(NS)]^+$, *cis*-$[Os^{IV}{-}NPPh_3]^+$, *cis*-$[Os^{IV}(tpy)(Cl)_2(NPPh_3)]^+$, tpy, 2,2′:6′,2″-terpyridine; triphenylphosphine sulfide, $SPPh_3$; TBAH, tetra-*n*-butylammonium hexafluorophosphate.

Experimental Section

Materials. House-distilled water was purified with a Barnstead E-Pure deionization system. High-purity acetonitrile was used as received from Burdick & Jackson. Osmium tetraoxide (>99%) was

† Current address: Associate Laboratory Director for Strategic and Supporting Research, Los Alamos National Laboratory, MS A127, Los Alamos, NM 87545. E-mail: tjmeyer@lanl.gov. Phone: 1-505-667-8597. Fax: 1-505-667-5450.

(1) El-Samanody, E.-S.; Demadis, K. D.; Gallagher, L. A.; Meyer, T. J.; White, P. S. *Inorg. Chem.* **1999**, *38*, 3329.

(2) (a) Bakir, M.; Dovletoglou, A.; White, P. S.; Meyer, T. J. *Inorg. Chem.* **1991**, *30*, 2835. (b) Demadis, K. D.; Bakir, M.; Klesczewski, B. G.; William, D. S.; Meyer, T. J.; White, P. S. *Inorg. Chim. Acta* **1998**, *270*, 511.

10.1021/ic991425t CCC: $19.00
Published on Web 06/09/2000

purchased from Alfa-AESAR. $SPPh_3$ was purchased from Aldrich and used without further purification. TBAH was recrystallized three times from boiling ethanol and dried under vacuum at 120 °C for 2 days. Common laboratory chemicals employed in the preparation of compounds were of reagent grade and were used without further purification.

Instrumentation and Measurements. FTIR, ^{1}H NMR, UV−visible, and near-IR spectroscopy, elemental analyses, cyclic voltammetry, and kinetic studies with UV−visible monitoring were performed similarly to those of ref 1. All kinetic studies were performed in CH_3CN at 25.0 ± 0.1 °C with pseudo-first-order excesses of $SPPh_3$ and PPh_3. The concentrations of solutions containing $[Os^{VI}{\equiv}N]^+$ were 8.16×10^{-6} M for *trans*-$[Os^{VI}{\equiv}N]^+$ and 4.90×10^{-5} M for *cis*-$[Os^{VI}{\equiv}N]^+$. The concentrations of $SPPh_3$ were varied from 6.70×10^{-5} to 6.70×10^{-4} M for *trans*-$[Os^{VI}{\equiv}N]^+$ and from 5.72×10^{-4} to 5.72×10^{-3} M for *cis*-$[Os^{VI}{\equiv}N]^+$. The concentrations of solutions containing $[Os^{II}{-}NS]^+$ were 1.05×10^{-5} M for *trans*-$[Os^{II}{-}NS]^+$ and 1.35×10^{-5} M for *cis*-$[Os^{II}{-}NS]^+$. The concentrations of PPh_3 were varied from 1.16×10^{-4} to 1.16×10^{-3} M for *trans*-$[Os^{II}{-}NS]^+$ and from 1.62×10^{-4} to 1.62×10^{-3} M for *cis*-$[Os^{II}{-}NS]^+$. All rate constants cited in this work are reported as the averages of at least three independent experiments.

Synthesis and Characterization. The following complexes and compounds were prepared by literature procedures: *trans*-$[Os^{VI}(tpy)(Cl)_2(N)](PF_6)$,[3] *trans*-$[Os^{II}(tpy)(Cl)_2(NS)](PF_6)$,[4] *trans*-$[Os^{IV}(tpy)(Cl)_2(NPPh_3)](PF_6)$,[2] and *cis*-$[Os^{VI}(tpy)(Cl)_2(N)](PF_6)$.[3]

***cis*-$[Os^{II}(tpy)(Cl)_2(NS)](PF_6)$ and *cis*-$[Os^{IV}(tpy)(Cl)_2(NPPh_3)](PF_6)$.** In a two-necked, round-bottom flask, *cis*-$[Os^{VI}(tpy)(Cl)_2(N)]^+$ (300 mg, 0.459 mmol) was stirred in 150 mL of CH_3CN under an argon atmosphere for 15 min. A 1.1 equiv amount of $SPPh_3$ (150 mg, 0.509 mmol) in 20 mL of CH_3CN was bubbled with argon for 5 min and added to the *cis*-$[Os^{VI}(tpy)(Cl)_2(N)]^+$ solution through a pressure-equalizing dropping funnel. The reaction mixture was continuously stirred under argon for 3 h, after which it was filtered through a fine frit. The brown filtrate was reduced to a small volume by rotary evaporation, and the concentrate was chilled in an ice bath for 1 h to precipitate a solid that was identified as *cis*-$[Os^{II}(tpy)(Cl)_2(NS)](PF_6)$. Upon addition of Et_2O to the concentrated filtrate, a second solid, *cis*-$[Os^{IV}(tpy)(Cl)_2(NPPh_3)](PF_6)$, was obtained and recrystallized from CH_3CN/Et_2O.

cis-$[Os^{II}(tpy)(Cl)_2(NS)](PF_6)$: yield 0.126 g (40.0%). Anal. Calcd for $OsC_{15}H_{11}N_4Cl_2SPF_6$: C, 26.29; H, 1.62; N, 8.17. Found: C, 26.40; H, 1.73; N, 8.25.

cis-$[Os^{IV}(tpy)(Cl)_2(NPPh_3)](PF_6)$: yield 0.192 g (45.7%). Anal. Calcd for $OsC_{33}H_{26}N_4Cl_2P_2F_6$: C, 43.29; H, 2.86; N, 6.12. Found: C, 43.18; H, 2.73; N, 6.23. Infrared data (cm^{-1}; KBr disks): $\nu(^{14}N{=}P)$ 1112 (vs); ν(tpy) 1474 (vs), 1449 (vs), 1384 (vs). UV−vis data [CH_3CN; λ_{max}, nm (ϵ, M^{-1} cm^{-1})]: 724 (310); 484 (2.18×10^3); 464 (2.40×10^3); 406 (2.75×10^3); 364 (9.77×10^3); 318 (2.05×10^4); 276 (3.00×10^4); 236 (4.59×10^4); 216 (4.83×10^4). Cyclic voltammetry data: $E_{1/2} = 1.06$ V (Os(IV/III)) and $E_{1/2} = -0.16$ V (Os(III/II)) vs SSCE in 0.1 M TBAH/CH_3CN.

***cis*-$[Os^{II}(tpy)(Cl)_2(NS)](SCN)$.** A 100 mg (46 μmol) quantity of *cis*-$[Os^{VI}(tpy)(Cl)_2(N)]^+$ was dissolved in 15 mL of acetone and 60 mL of CS_2. A solution of $(PPN)N_3$ (PPN^+ = bis(triphenylphosphoranylidene)-ammonium cation) (27 mg, 46 mmol) in 15 mL of acetone was added dropwise to the mixture under stirring. The brown reaction mixture was stirred at room temperature for 2 h, during which a brown solid formed. This solid was filtered off, washed with acetone and Et_2O, and recrystallized from CH_3CN/Et_2O: yield 78.6 mg (85.8%). Anal. Calcd for $OsC_{16}H_{11}N_5Cl_2S_2{\cdot}1.5H_2O$: C, 30.72; H, 2.26; N, 11.02. Found: C, 31.05; H, 2.22; N, 10.55. UV−vis data [CH_3CN; λ_{max}, nm (ϵ, M^{-1} cm^{-1})]: 603 (400); 410 (1.20×10^3); 362 (8.45×10^3); 346 (9.63×10^3); 274 (2.69×10^4); 238 (3.54×10^4); 216 (3.60×10^4). Infrared data (cm^{-1}; KBr disk): ν(tpy) 1473 (vs), 1450 (vs), 1397 (vs); ν(N≡S) 1287; ν(SCN) 2045. Cyclic voltammetry data: $E_{1/2} = -0.09$ V ($NS^+ \rightarrow NS^{\bullet}$), $E_{1/2} = -0.28$ V ($NS^{\bullet} \rightarrow NS^-$), and $E_{1/2} = 0.97$ V (Os(III/II)) vs SSCE in 0.1 M TBAH, 1:1 (v/v) DMF/CH_3CN.

Table 1. Summary of Crystal Data, Intensity Collection Details, and Structure Refinement Parameters for *cis*-$[Os^{IV}(tpy)(Cl)_2(NPPh_3)](PF_6)$

empirical formula	$OsC_{33}H_{26}N_4Cl_2P_2F_6$
mol wt	915.63
a (Å)	9.2444(4)
b (Å)	17.6325(8)
c (Å)	20.1026(9)
β (Å)	91.310(1)
V (Å^3)	3275.9(3)
Z	4
crystal system	monoclinic
space group	$P2_1/c$
crystal size (mm)	$0.40 \times 0.05 \times 0.05$
d_{calcd} (g/cm^3)	1.857
diffractometer	Siemens CCD Smart
radiation; λ (Å)	Mo Kα; 0.710 73
collcn temp (°C)	−100
abs coeff, μ (cm^{-1})	5.75
F(000)	1783.63
$2\theta_{max}$ (deg)	50.0
no. of tot. reflns	14 004
no. of unique reflns	5771
no. of refined reflns	4222
merging R value	0.037
no. of params	434
R (%)[a]	0.059
R_w (%)[b]	0.045
goodness of fit[c]	0.000
deepest hole (e/Å^3)	−1.750
highest peak (e/Å^3)	1.980
σ	0.0549

[a] $R = \sum|F_o - F_c|/\sum|F_o|$. [b] $R_w = [\sum w(F_o - F_c)^2/\sum wF_o^2]^{1/2}$. [c] GoF = $[\sum w(F_o - F_c)^2/(\text{no. of reflns} - \text{no. of params})]^{1/2}$.

X-ray Structural Determination. Single crystals of *cis*-$[Os^{IV}(tpy)(Cl)_2(NPPh_3)](PF_6)$ were obtained by slow diffusion of Et_2O into a CH_3CN solution. Crystal data, intensity collection details, and structure refinement parameters are listed in Table 1. The structure was solved by direct methods. The remaining non-hydrogen atoms were located in subsequent difference Fourier maps. Empirical absorption corrections were applied with SADABS. The ORTEP plotting program was used to computer-generate the structure shown in Figure 1.[5] Hydrogen atoms were included in calculated positions with thermal parameters derived from the atoms to which they were bonded. All computations were performed by using the NRCVAX suite of programs.[6] Atomic scattering factors were taken from a standard source[7] and corrected for anomalous dispersion. The final positional parameters along with their standard deviations as estimates from the inverse matrix, hydrogen atom parameters, thermal parameters, and bond distances and angles for *cis*-$[Os^{IV}(tpy)(Cl)_2(NPPh_3)](PF_6)$ are available as Supporting Information. Selected bond distances and angles for the cation are listed in Tables 2 and 3, respectively.

Results

Synthesis and Mechanism of Formation. In the preparations of *cis*-$[Os^{II}(tpy)(Cl)_2(NS)]^+$ and *cis*-$[Os^{IV}(tpy)(Cl)_2(NPPh_3)]^+$, stoichiometric addition of triphenylphosphine sulfide in CH_3CN (1.53×10^{-2} M) to *cis*-$[Os^{VI}(tpy)(Cl)_2(N)]^+$ in CH_3CN (2.55×10^{-3} M) resulted in a color change from brown to darker brown within 20 min. After 3 h of stirring, the brown solution

(3) (a) Ware, D. C.; Taube, H. *Inorg. Chem.* **1991**, *30*, 4598. (b) Pipes, D. W.; Bakir, M.; Vitols, S. E.; Hodgson, D. J.; Meyer, T. J. *J. Am. Chem. Soc.* **1990**, *112*, 5507.
(4) (a) Demadis, K. D.; El-Samanody, E.-S.; Meyer, T. J.; White, P. S. *Inorg. Chem.* **1998**, *37*, 838. (b) Demadis, K. D.; Meyer, T. J.; White, P. S. *Inorg. Chem.* **1998**, *37*, 3610.
(5) Johnson, C. K. *ORTEP*: *A Fortran Thermal Ellipsoid Plot Program*; Technical Report ORNL-5138; Oak Ridge National Laboratory: Oak Ridge, TN, 1976.
(6) Gabe, E. J.; Le Page, Y.; Charland, J.-P.; Lee, F. L.; White, P. S. *J. Appl. Crystallogr.* **1989**, *22*, 384.
(7) *International Tables for X-ray Crystallography*; Kynoch Press: Birmingham, U.K., 1974; Vol. IV.

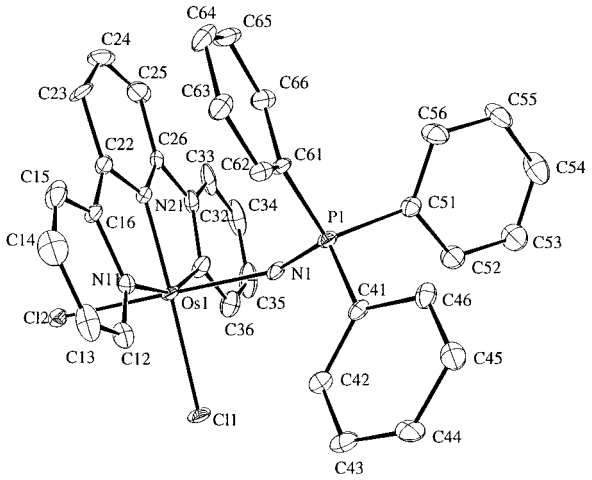

Figure 1. ORTEP diagram (30% ellipsoids) and labeling scheme for the cation *cis*-$[Os^{VI}(tpy)(Cl)_2(NPPh_3)]^+$ in the PF_6^- salt.

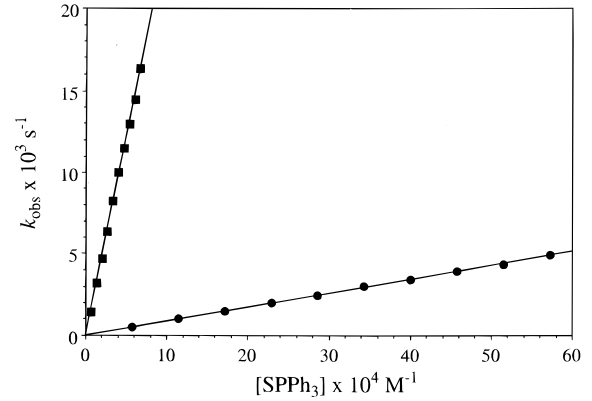

Figure 2. Plots of k_{obs} versus [$SPPh_3$] for the formations of *cis*-$[Os^{IV}(tpy)(Cl)_2(NPPh_3)](PF_6)$ (○) and *trans*-$[Os^{IV}(tpy)(Cl)_2(NPPh_3)](PF_6)$ (■) in CH_3CN at 25.0 ± 0.1 °C.

was reduced to a small volume and then chilled in an ice−water bath for 1 h. The PF_6^- salt of *cis*-$[Os^{II}(tpy)(Cl)_2(NS)]^+$ that precipitated was filtered off, washed with a small amount of cold CH_3CN, and air-dried. The filtrate was further concentrated and added dropwise to Et_2O to precipitate the PF_6^- salt of *cis*-$[Os^{IV}(tpy)(Cl)_2(NPPh_3)]^+$, which was recrystallized from CH_3CN/Et_2O.

Reaction between *cis*-$[Os^{VI}(tpy)(Cl)_2(N)]^+$ and $SPPh_3$ provides a useful synthetic route to *cis*-$[Os^{II}(tpy)(Cl)_2(NS)]^+$ and *cis*-$[Os^{IV}(tpy)(Cl)_2(NPPh_3)]^+$, which were previously unknown. The structure of *cis*-$[Os^{IV}(tpy)(Cl)_2(NPPh_3)]^+$ is shown in Figure 1. This is also a convenient synthetic procedure for *trans*-$[Os^{II}(tpy)(Cl)_2(NS)]^+$ compared to the earlier reaction involving N_3^- and CS_2.[4b] $SPPh_3$ may be a useful reagent for the preparation of other metal−thionitrosyl complexes from metal−nitrido complexes.

Kinetics. The kinetics and stoichiometry of the reactions between *cis*- and *trans*-$[Os^{VI}(tpy)(Cl)_2(N)]^+$ and $SPPh_3$ were studied in CH_3CN at 25.0 ± 0.1 °C by following characteristic changes in the absorption spectra of $[Os^{VI}(tpy)(Cl)_2(N)]^+$ under pseudo-first-order conditions in $SPPh_3$. As shown by the plots of k_{obs} vs [$SPPh_3$] in Figure 2, the kinetics are first order in $SPPh_3$, consistent with the rate law

$$\frac{-d[Os^{VI}{\equiv}N^+]}{dt} = k[Os^{VI}{\equiv}N^+][SPPh_3] = k_{obs}[Os^{VI}{\equiv}N^+]$$

with $k_{obs} = k[SPPh_3]$. Each rate constant in Figure 2 is the average of three independent experiments. On the basis of the experimental slopes and the above rate law, k_{trans}(25 °C, CH_3CN) = 24.6 ± 0.6 M^{-1} s^{-1} and k_{cis}(25 °C, CH_3CN) = 0.84 ± 0.09 M^{-1} s^{-1}.

A rapid reaction occurs upon mixing excess PPh_3 and $[Os^{II}(tpy)(Cl)_2(NS)]^+$ in CH_3CN. The products of the reaction were determined to be $[Os^{IV}(tpy)(Cl)_2(NPPh_3)]^+$ by UV−visible measurements at 470, 412, and 354 nm and $SPPh_3$ by IR with characteristic bands at 1434 (vs), 1306, 1103 (vs), 714, and 517 cm^{-1} matched to those of an authentic sample (Aldrich).[1] On the basis of the results of a kinetics study with UV−visible monitoring, the rate law was first order in each reagent:

$$\frac{-d[Os^{II}{-}NS^+]}{dt} = k[Os^{II}{-}NS^+][PPh_3] = k_{obs}[Os^{II}{-}NS^+]$$

with $k_{obs} = k[PPh_3]$. From the slope of a plot of k_{obs} vs [PPh_3], k_{trans}(25 °C, CH_3CN) = (6.79 ± 0.08) × 10^2 M^{-1} s^{-1} and k_{cis}(25 °C, CH_3CN) = (2.30 ± 0.07) × 10^2 M^{-1} s^{-1}.

^{1}H NMR Spectroscopy. The ^{1}H NMR spectrum of *cis*-$[Os^{IV}(tpy)(Cl)_2(NPPh_3)]^+$ shows that the complex is diamagnetic, with resonances for the aromatic protons from the tpy and PPh_3 ligands appearing from 7.35 to 10.54 ppm. Earlier ^{1}H NMR measurements on *trans*-$[Os^{IV}(tpy)(Cl)_2(NPPh_3)]^+$ revealed that it is paramagnetic.[2b] As expected, *trans*- and *cis*-$[Os^{II}(tpy)(Cl)_2(NS)]^+$ are diamagnetic. For *trans*-$[Os^{II}(tpy)(Cl)_2(NS)]^+$, aromatic protons for the tpy ligand appear at 7.91−7.95 ppm (triplet of 5- and 5″-protons), 8.16−8.22 ppm (triplet of 4- and 4″-protons), 8.47−8.52 ppm (triplet of 4′-protons), 8.53−8.59 ppm (doublet of 3-, 3′-, 5′-, and 3″-protons), and 8.72−8.75 ppm (doublet of 6- and 6″-protons). The protons of the tpy ligand in *cis*-$[Os^{II}(tpy)(Cl)_2(NS)]^+$ appeared in a similar pattern: 8.06−8.10 ppm (triplet of 5- and 5″-protons), 8.51−8.57 ppm (triplet of 4- and 4″-protons), 8.73−8.78 ppm (triplet of 4′-protons), 8.97−9.00 ppm (doublet of 3-, 3′-, 5′-, and 3″-protons), and 9.29−9.30 ppm (doublet of 6- and 6″-protons).

UV−Visible Spectroscopy. The UV spectrum of *cis*-$[Os^{IV}(tpy)(Cl)_2(NPPh_3)]^+$ is dominated by intense $\pi \rightarrow \pi^*$(tpy) bands at 318, 276, 236, and 216 nm and a band for the phenyl-containing phosphoraniminato ligand at 280 nm. A series of relatively intense charge-transfer bands appear in the visible region at 724, 484, 464, 406, and 364 nm, and two weak interconfigurational (IC) $d\pi \rightarrow d\pi$ bands appear in the near-IR region at 1765 and 1913 nm.

Ligand-to-metal charge-transfer bands (LMCT) arising from $Cl^- \rightarrow Os^{IV}$ charge transfer in *trans*-$[Os^{IV}(PEt_3)_2(Cl)_4]$ have been assigned at 465 and 380 nm. $E_{1/2}(Os^{IV/III})$ = 0.33 V (vs SSCE in CH_2Cl_2) for this complex[2b,8] compared to −0.10 V for *cis*-$[Os^{IV}(tpy)(Cl)_2(NPPh_3)]^+$, consistent with the assignment of the bands at 406 and 364 nm for the latter to ligand-to-metal charge-transfer (LMCT) transitions from Cl^- or $NPPh_3^-$ to Os(IV).

The visible absorption bands at 724, 484, and 464 nm can be assigned to metal-to-ligand charge-transfer (MLCT) $d\pi \rightarrow \pi^*$(tpy) bands.[2b] The MLCT assignments are reasonable on energetic grounds. For example, for *trans*-$[Os^{II}(tpy)(Cl)_2(4\text{-}(CH_3)_3Cpy)]$,[4b] λ_{max} occurs at 500 nm with $E_{1/2}(Os^{III/II})$ = 0.02 V (vs SSCE in CH_3CN) compared to λ_{max} at 484 nm and $E_{1/2}(Os^{IV/III})$ = −0.10 V for *cis*-$[Os^{IV}(tpy)(Cl)_2(NPPh_3)]^+$. The $E_{1/2}$ value for the Os(IV/III) couple shows that the $d\pi-\pi^*$(tpy) energy gap is comparable to that for the Os(II) complex since π^*_1(tpy) is the common acceptor level in both complexes.[4b] Molar absorptivities are lower than those for typical Os(II) MLCT absorption bands, consistent with less $d\pi$(Os(IV) → π^*(tpy)) overlap as expected for the higher oxidation state.

Table 2. Selected Bond Lengths (Å) for *cis*-[Os^{IV}(tpy)$(Cl)_2$(NPPh$_3$)](PF_6)

Os(1)-Cl(1)	2.3780(17)	N(11)-C(16)	1.403(10)	C(25)-C(26)	1.370(12)
Os(1)-Cl(2)	2.3714(20)	C(12)-C(13)	1.383(13)	C(26)-C(32)	1.506(13)
Os(1)-N(1)	2.071(6)	C(13)-C(14)	1.370(15)	N(31)-C(32)	1.384(11)
Os(1)-N(11)	2.077(6)	C(14)-C(15)	1.382(16)	N(31)-C(36)	1.341(11)
Os(1)-N(21)	1.943(6)	C(15)-C(16)	1.380(13)	C(32)-C(33)	1.383(13)
Os(1)-N(31)	2.064(7)	C(16)-C(22)	1.464(13)	C(33)-C(34)	1.367(18)
P(1)-N(1)	1.619(7)	N(21)-C(22)	1.390(10)	C(34)-C(35)	1.400(18)
P(1)-C(41)	1.788(8)	N(21)-C(26)	1.329(11)	C(35)-C(36)	1.385(14)
P(1)-C(51)	1.784(8)	C(22)-C(23)	1.402(11)	C(41)-C(42)	1.402(11)
P(1)-C(61)	1.7792(7)	C(23)-C(24)	1.369(18)	C(41)-C(46)	1.406(11)
N(11)-C(12)	1.315(11)	C(24)-C(25)	1.378(18)	C(42)-C(43)	1.385(12)
C(43)-C(44)	1.375(14)	C(44)-C(45)	1.383(12)	C(45)-C(46)	1.384(12)
C(51)-C(52)	1.397(11)	C(51)-C(56)	1.403(11)	C(52)-C(53)	1.374(13)
C(53)-C(54)	1.384(14)	C(54)-C(55)	1.382(13)	C(55)-C(56)	1.385(13)
C(61)-C(62)	1.384(12)	C(61)-C(66)	1.411(11)	C(62)-C(63)	1.392(11)
C(63)-C(64)	1.392(12)	C(64)-C(65)	1.383(13)	C(65)-C(66)	1.381(11)

Table 3. Selected Bond Angles (deg) for *cis*-[Os^{IV}(tpy)$(Cl)_2$(NPPh$_3$)](PF_6)

Cl(1)-Os(1)-N(11)	100.25(18)	Cl(1)-Os(1)-Cl(2)	91.02(7)	C(16)-C(22)-N(21)	113.5(6)
Cl(1)-Os(1)-N(1)	88.36(17)	Os(1)-N(31)-C(36)	129.2(6)	C(22)-N(21)-C(26)	120.5(7)
Cl(1)-Os(1)-N(21)	177.26(21)	P(1)-C(51)-C(56)	125.2(6)	C(13)-C (14)-C(15)	119.2(9)
Cl(1)-Os(1)-N(31)	99.34(19)	N(21)-C(26)-C(25)	122.5(9)	N(11)-C(16)-C(15)	119.4(8)
Cl(2)-Os(1)-N(1)	174.58(18)	C(23)-C(24)-C(25)	121.1(8)	N(11)-C(16)-C(22)	115.1(7)
Cl(2)-Os(1)-N(11)	88.31(18)	N(21)-C(26)-C(32)	111.4(7)	C(14)-C(15)-C(16)	120.7(8)
Cl(2)-Os(1)-N(21)	86.57(20)	C(22)-C(23)-C(24)	119.7(9)	Os(1)-N(21)-C(22)	117.9(5)
Cl(2)-Os(1)-N(31)	90.99(20)	C(24)-C(25)-C(26)	118.0(9)	Os(1)-N(21)-C(26)	121.4(5)
N(1)-Os(1)-N(11)	97.10(25)	C(32)-N(31)-C(36)	117.4(7)	C(51)-P(1)-C(61)	110.5(4)
N(1)-Os(1)-N(21)	93.92(25)	N(21)-C(22)-C(23)	118.0(8)	C(41)-P(1)-C(61)	106.2(4)
N(l)-Os(1)-N(31)	83.8(3)	N(21)-Os(1)-N(31)	79.4(3)	C(33)-C(34)-C(35)	119.3(9)
N(11)-Os(1)-N(21)	81.0(3)	Os(1)-N(1)-P(1)	138.4(4)	C(41)-P(1)-C(51)	104.0(4)
N(11)-Os(1)-N(31)	160.4(3)	Os(1)-N(11)-C(12)	129.5(5)	P(1)-C(41)-C(42)	120.1(6)
Os(1)-N(31)-C(32)	113.3(5)	Os(1)-N(11)-C(16)	112.1(5)	P(1)-C(41)-C(46)	120.6(6)
N(1)-P(1)-C(51)	109.0(4)	N(1)-P(1)-C(41)	115.1(3)	C(41)-C(42)-C(43)	120.2(8)
C(44)-C(45)-C(46)	120.0(8)	C(42)-C(41)-C(46)	119.3(7)	C(42)-C(43)-C(44)	119.7(8)
C(41)-C(46)-C(45)	119.7(8)	C(26)-C(32)-N(31)	114.3(17)	C(43)-C(44)-C(45)	121.1(9)
C(26)-C(32)-C(33)	124.1(8)	C(34)-C(35)-C(36)	118.2(9)	N(31)-C(36)-C(35)	123.5(9)
N(31)-C(32)-C(33)	121.5(9)	C(32)-C(33)-C(34)	120.0(9)	C(25)-C(26)-C(32)	126.0(9)
P(1)-C(51)-C(56)	125.2(6)	C(52)-C(51)-C(56)	118.0(8)	C(51)-C(52)-C(53)	121.1(8)
C(52)-C(53)-C(54)	120.4(8)	C(53)-C(54)-C(55)	119.6(8)	C(54)-C(55)-C(56)	120.4(8)
C(51)-C(56)-C(55)	120.5(8)	P(1)-C(61)-C(62)	121.5(6)	P(1)-C(61)-C(66)	119.1(6)
C(62)-C(61)-C(66)	119.4(7)	C(61)-C(62)-C(63)	120.4(7)	C(62)-C(63)-C(64)	119.6(8)
C(63)-C(64)-C(65)	120.3(7)	C(64)-C(65)-C(66)	120.3(7)	C(61)-C(66)-C(65)	119.9(8)

Given the ground-state configuration $d\pi_1^2 d\pi_2^2 d\pi_3^0$, the IC bands at 1765 and 1913 nm can be assigned to the transitions $d\pi_1^2 d\pi_2^2 d\pi_3^0 \rightarrow d\pi_1^1 d\pi_2^2 d\pi_3^1$ and $d\pi_1^2 d\pi_2^2 d\pi_3^0 \rightarrow d\pi_1^2 d\pi_2^1 d\pi_3^1$, respectively.[2b]

The UV spectral region for *cis*-[Os^{II}(tpy)$(Cl)_2$(NS)]$^+$ is dominated by intense $\pi-\pi^*$(tpy) bands at 274, 238, and 216 nm. Bands of relatively low intensity appear at 603, 410, 362, and 346 nm. Defining the $Os^{II}-NS$ bond to lie along the molecular *z* axis, we can assign the bands at 603 and 410 nm to the Os(II) $\rightarrow$ NS MLCT transitions $d_{xy} \rightarrow \pi_1^*$(NS) and $d_{xy} \rightarrow \pi_2^*$(NS), respectively.[1,9] For the trans isomer, $\pi \rightarrow \pi^*$(tpy) bands appear at 280, 244, and 218 nm and $d_{xy} \rightarrow \pi^*$(NS) bands at 658 and 434 nm. These data were summarized in the Experimental Section.

Infrared Spectroscopy. Both symmetrical and unsymmetrical vibrations of the Os−N═P unit in *cis*-[Os^{IV}(tpy)$(Cl)_2$(NPPh$_3$)](PF_6) are observed in KBr, with ν(N═P) appearing at 1112 cm^{-1}. The range for other Os−phosphoraniminato complexes is 1100−1120 cm^{-1}.[2] An intense PF_6^- band appears at 841 cm^{-1}, and intense bands for tpy appear at 1474 (vs), 1449 (vs), and 1384 (vs) cm^{-1}.

In the spectrum of *cis*-[Os^{IV}(tpy)$(Cl)_2$(NS)](SCN), an intense band for ν(N≡S) appears at 1287 cm^{-1}, which is in the normal range of 1150−1400 cm^{-1} found for related complexes.[10] An intense band appears at 2045 cm^{-1} for ν(SCN), and intense bands at 1473, 1450, and 1397 have their origin in the tpy ligand.

Redox Properties. In cyclic voltammograms of *cis*-[Os^{IV}(tpy)$(Cl)_2$(NPPh$_3$)]$^+$ in 0.1 M TBAH/CH_3CN, waves appear at $E_{1/2}$ = 1.06 and −0.16 V (vs SSCE), arising from Os(V/IV) and Os(IV/III) couples. There is no evidence for an Os(III/II) wave to the solvent limit. For comparison, $E_{1/2}(Os^{V/IV}) = 0.92$ V and $E_{1/2}(Os^{IV/III}) = -0.27$ V for the trans isomer.[2b]

In 0.1 M TBAH, 1:1 (v/v) DMF/CH_3CN, reduction of *trans*-[Os^{II}(tpy)$(Cl)_2$(NS)]$^+$ occurs at $E_{1/2} = 0.0$ and −0.21 V. In the same solvent, reduction of the cis isomer gives chemically quasi-reversible couples at $E_{1/2} = -0.09$V and −0.28 V. These reduction waves appear to be associated with thionitrosyl ligand-based reductions. Analogous waves have been reported for *trans*-[Os^{II}(tpy)$(Cl)_2$(NO)]$^+$ and [Os^{II}(tpm)$(Cl)_2$(NS)]$^+$.[1,11] On the reverse, oxidative, scan, there is evidence for a reversible oxidation of the trans isomer at 0.91 V and a quasi-reversible oxidation of the cis isomer at 0.97 V.

(8) Cipriano, R. A.; Levason, W.; Mould, R. A. S.; Pletcher, D.; Webester, M. *J. Chem. Soc., Dalton Trans.* **1990**, 339.

(9) With the $Os^{II}-NS$ bond axis defined as the *z* axis, $d\pi \rightarrow \pi^*$(NS) mixing is dominated by the d_{xz} and d_{yz} orbitals. The d_{xy} orbital is orthogonal to these interactions.[1]

(10) (a) Roesky, H. W.; Pandey, K. K. *Adv. Inorg. Chem. Radiochem.* **1983**, *26*, 337 and references therein. (b) Pandey, K. K. *Prog. Inorg. Chem.* **1992**, *40*, 445 and references therein.

(11) (a) Murphy, W. R., Jr.; Takeuchi, K. J.; Meyer, T. J. *J. Am. Chem. Soc.* **1982**, *104*, 517. (b) Ooyama, D.; Nagao, H.; Ito, K.; Nagao, N.; Howell, F. S.; Mukaida, M. *Bull. Chem. Soc. Jpn.* **1997**, *70*, 2141.

Scheme 1

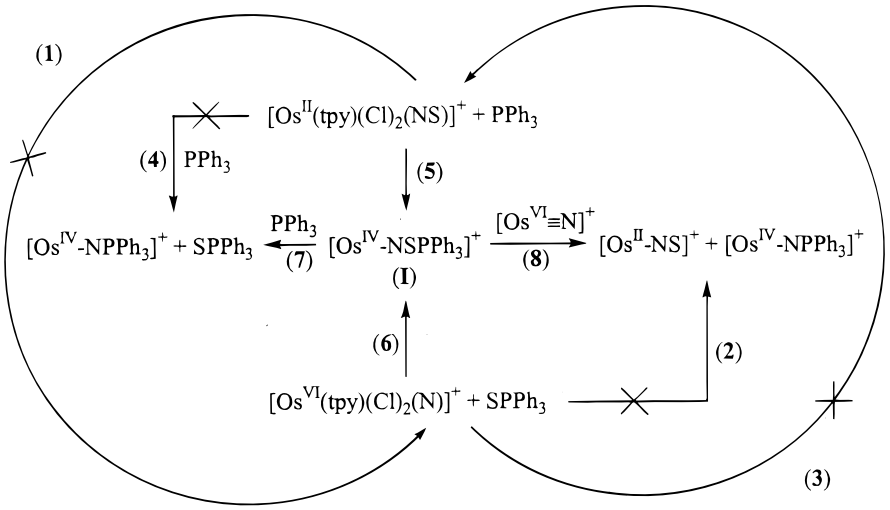

Structure and Bonding. An ORTEP diagram of the cation *cis*-$[Os^{IV}(tpy)(Cl)_2(NPPh_3)]^+$ with a labeling scheme is presented in Figure 1. The crystal contains discrete *cis*-$[Os^{IV}(tpy)(Cl)_2(NPPh_3)]^+$ cations and PF_6^- anions. The Cl^- ligands remain in the cis configuration of the parent nitrido complex. There is evidence in the structure of *cis*-$[Os^{VI}(tpy)(Cl)_2(N)]^+$ for a trans effect due to the nitrido ligand with the bond length of Os−Cl trans to the nitrido ligand being 2.518(1) Å and the bond length of Os−Cl trans to tpy being 2.357(1) Å.[12] There is no evidence for a trans effect in *cis*-$[Os^{IV}(tpy)(Cl)_2(NPPh_3)]^+$. The Os−Cl bond lengths are 2.378(2) and 2.371(2) Å, nearly the same as the length of Os−Cl trans to tpy in the parent nitrido complex, 2.357(1) Å. The P═N bond length of 1.619(7) Å lies within the normal range of 1.503−1.656 Å.[2b,14] The Cl−Os−N(tpy) and Cl−Os−N(PPh_3) angles are near 180° at 177.26(21) and 174.58(18)°. The Os−N−P angle of 138.4(4)° is in the lower range of M−N−P angles, 125.3−180°.[15]

There is no evidence for a trans influence due to $NPPh_3^-$ or for Os−N multiple bonding. The Os−N(PPh_3) bond length is 2.071(6) Å, which is in the upper range of M−NPR_3 bond lengths (1.65−2.33 Å) and is indicative of a bond order of 1.[2b,13] This and the Os−N(PPh_3) bond length in the cis isomer (2.071 Å) are comparable to the Os−N bond lengths of the noncentral pyridyl rings (2.064−2.081 Å) of the tpy ligand. These bond lengths are relatively isomer independent and consistent with a single bond. The acute Os−N−P angle of 138.4(4)° is also consistent with the absence of significant Os−N(PPh_3) multiple bonding.[2b] This is true even though there are well-established examples of M−N multiple bonding,[14b] including a Ti−N bond length of 1.734(3) Å and a Ti−N−P angle of 160.0(2)° in $[Ti^{IV}(Cl)_3(NPEt_3)(THF)_2]$ consistent with double bonding[16] and a V−N bond length of 1.653(3) Å and a V−N−P angle of 171.8(2)° in $[V^V(NPMePh_2)(Cl)_4(NCCH_3)]$ consistent with triple bonding.[17]

Discussion

In an earlier study, $[Os^{II}(tpm)(Cl)_2(NS)]^+$ was shown to react with PPh_3 to give $[Os^{IV}(tpm)(Cl)_2(NPPh_3)]^+$ and $SPPh_3$ by a rate law first order in both reagents.[1] In this study, we report the analogous reactions of *cis*- and *trans*-$[Os^{II}(tpy)(Cl)_2(NS)]^+$ with PPh_3 to give $[Os^{IV}(tpy)(Cl)_2(NPPh_3)]^+$ and $SPPh_3$, eq 5,

$$[Os^{II}(tpy)(Cl)_2(NS)]^+ + 2PPh_3 \rightarrow [Os^{IV}(tpy)(Cl)_2(NPPh_3)]^+ + SPPh_3 \quad (5)$$

as well as reactions of *cis*- and *trans*-$[Os^{VI}(tpy)(Cl)_2(N)]^+$ with $SPPh_3$ to give $[Os^{IV}(tpy)(Cl)_2(NPPh_3)]^+$ and $[Os^{II}(tpy)(Cl)_2(NS)]^+$, eq 4.

At first glance, these two reactions seem incompatible. In eq 5, a reaction occurs between $[Os^{II}(tpy)(Cl)_2(NS)]^+$ and PPh_3 that results in net S atom transfer to PPh_3. In eq 4, a reaction occurs between $[Os^{VI}(tpy)(Cl)_2(N)]^+$ and $SPPh_3$ that results in net S atom transfer in the opposite sense to give $[Os^{II}(tpy)(Cl)_2(NS)]^+$ and $[Os^{IV}(tpy)(Cl)_2(NPPh_3)]^+$. The reaction in eq 4 is energetically favored because of the formation of the coproduct, $[Os^{IV}(tpy)(Cl)_2(NPPh_3)]^+$.

The fact that both of these reactions occur shows that neither occurs by a simple S atom transfer mechanism. The results can be explained by invoking a common intermediate, $[Os^{IV}(tpy)(Cl)_2(NSPPh_3)]^+$. A proposed mechanism is shown in Scheme 1.

If the reaction between $[Os^{II}(tpy)(Cl)_2(NS)]^+$ and PPh_3 occurred by a S atom transfer mechanism (reaction 4) and path 1 in Scheme 1, the initial products would be $[Os^{VI}(tpy)(Cl)_2(N)]^+$ and $SPPh_3$. Once formed, they would undergo the reaction in path 2 of Scheme 1 to give $[Os^{IV}(tpy)(Cl)_2(NPPh_3)]^+$ and $[Os^{II}(tpy)(Cl)_2(NS)]^+$. The actual products are $[Os^{IV}(tpy)(Cl)_2(NPPh_3)]^+$ and $SPPh_3$.

Similarly, if the reaction between $[Os^{VI}(tpy)(Cl)_2(N)]^+$ and $SPPh_3$ occurred by S atom transfer (reaction 2) and path 3 in Scheme 1, the initial products would be $[Os^{II}(tpy)(Cl)_2(NS)]^+$ and PPh_3 and the final products would be $[Os^{IV}(tpy)(Cl)_2(NPPh_3)]^+$ and $SPPh_3$ via path 4 in Scheme 1. The actual products are $[Os^{IV}(tpy)(Cl)_2(NPPh_3)]^+$ and $[Os^{II}(tpy)(Cl)_2(NS)]^+$.

(12) Huynh, M. H. V.; White, P. S.; Meyer, T. J. Unpublished results, 1998.
(13) (a) Dehnicke, K.; Strähle, J. *Polyhedron* **1989**, 707. (b) Rübenstahl, T.; Well, F.; Harms, K.; Dehnicke, K.; Fenske, D.; Baum, G. *Z. Anorg. Allg. Chem.* **1994**, *620*, 1741.
(14) (a) Anfang, S.; Harms, K.; Dehnicke, K. Unpublished results, 1998. (b) Dehnicke, K.; Krieger, M.; Massa, W. *Coord. Chem. Rev.* **1999**, *182*, 19.
(15) (a) Nusshär, D.; Weller, F.; Dehnicke, K. *Z. Anorg. Allg. Chem.* **1993**, *619*, 1121. (b) Rübenstahl, T.; Wolff von Gudenberg, D.; Weller, F.; Dehnicke, K.; Goesmann, H. *Z. Naturforsch.* **1994**, *49B*, 15.
(16) Stahl, M. M.; Faza, N.; Massa, W.; Dehnicke, K. *Z. Anorg. Allg. Chem.* **1998**, *624*, 209.
(17) Schomber, B. M.; Ziller, J. W.; Doherty, N. M. *Inorg. Chem.* **1991**, *30*, 4488.

Both results can be explained by invoking a common intermediate, **I**, which forms via paths 5 and 6 in Scheme 1. Under the condition of the reaction between $[Os^{II}(tpy)(Cl)_2(NS)]^+$ and PPh_3, once **I** forms via path 5 in Scheme 1, it does not build up as an intermediate. Its subsequent reaction with PPh_3 via path 7 in Scheme 1 is more rapid than its formation. This is shown by the rate law which is first order in $[Os^{II}(tpy)(Cl)_2(NS)]^+$ and first order in PPh_3. $[Os^{VI}(tpy)(Cl)_2(N)]^+$ is not present in the solution, and only PPh_3 is available to capture **I**.

Similarly, in the formation of **I** via path 6 in Scheme 1, **I** does not build up as an intermediate. Its subsequent reaction with $[Os^{VI}(tpy)(Cl)_2(N)]^+$ via path 8 in Scheme 1 is more rapid than its formation as shown by the rate law. PPh_3 is not present, and only $[Os^{VI}(tpy)(Cl)_2(N)]^+$ is available to capture **I**.

It is not possible to conduct a convenient competition experiment, for example, by observing the product distribution in a reaction between $[Os^{VI}(tpy)(Cl)_2(N)]^+$ and $SPPh_3$ with added PPh_3 because the reaction between $[Os^{VI}(tpy)(Cl)_2(N)]^+$ and PPh_3 is too rapid with k(25 °C, CH_3CN) = (1.36 ± 0.08) × 10^4 M^{-1} s^{-1} for *trans*-$[Os^{VI}(tpy)(Cl)_2(N)]^+$.[2b]

Intermediate **I** can be viewed as an Os(IV) complex containing a N-bound monoanionic ligand which is either $SNPPh_3^-$ or $NSPPh_3^-$. There is precedent for the S−N−P core in the structure of $Ph_3P{=}N{-}SN_3S_2$.[18] Assuming the same for **I**, in a formal sense, the reaction between $[Os^{VI}(tpy)(Cl)_2(N)]^+$ and $SPPh_3$ involves net N^- transfer from the nitrido complex to $SPPh_3$:[19]

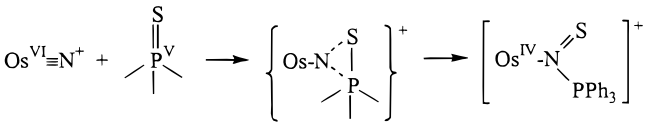

An important part of this reaction may be initial electron donation from a filled $d\pi$-p_N orbital, largely localized on the nitrido ligand,[20] to a π^*_{PS} orbital on $SPPh_3$.

The reaction between **I** and PPh_3 may involve initial electron donation from PPh_3 to a largely S-based π^*_{NS} orbital on $N(S)PPh_3^-$ followed by displacement of $SPPh_3$, eq 6.

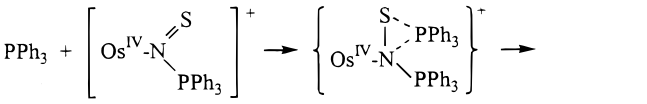

$$Os^{IV}\text{-}NPPh_3^+ + SPPh_3 \quad (6)$$

The reaction between **I** and $[Os^{VI}(tpy)(Cl)_2(N)]^+$ involves electrophilic displacement of the thionitrosyl complex by the nitrido complex, eq 7. There is presumably an initial electronic interaction between the P atom and vacant $d\pi^*_{OsN}$ orbitals, largely localized on the metal:

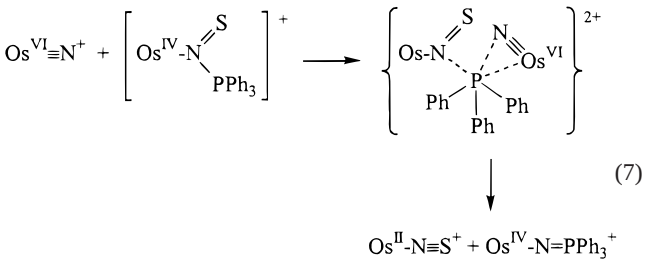

$$Os^{II}\text{-}N{\equiv}S^+ + Os^{IV}\text{-}N{=}PPh_3^+ \quad (7)$$

Electron pair donation from the P atom to the π^*_{NS} orbital is important in the reactions between *cis*- and *trans*-$[Os^{II}(tpy)(Cl)_2(NS)]^+$ and PPh_3, eq 8.

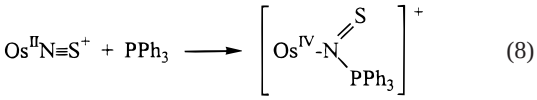

This can be inferred from the fact that the rate constant for *trans*-$[Os^{II}(tpy)(Cl)_2(NS)]^+$ (k_{trans}(25 °C, CH_3CN) = (6.79 ± 0.08) × 10^2 M^{-1} s^{-1}) is ∼3 times larger than that for *cis*-$[Os^{II}(tpy)(Cl)_2(NS)]^+$. This reactivity parallels the two-electron potentials for reduction of the NS^+ ligand, −0.11 and −0.19 V for *trans*-$[Os^{II}(tpy)(Cl)_2(NS)]^{+/-}$ and *cis*-$[Os^{II}(tpy)(Cl)_2(NS)]^{+/-}$ (0.1 M TBAH in 1:1 (v/v) DMF/CH_3CN, vs SSCE).[21]

The kinetics data for the reactions between *cis*- and *trans*-$[Os^{VI}(tpy)(Cl)_2(N)]^+$ with $SPPh_3$ are also revealing. Reaction with *trans*-$[Os^{VI}(tpy)(Cl)_2(N)]^+$ is ∼30 times faster than that with *cis*-$[Os^{VI}(tpy)(Cl)_2(N)]^+$ even though the order of the irreversible one-electron reduction potentials is the opposite with E_{pc} = −0.28 V for *cis*-$[Os^{VI}(tpy)(Cl)_2(N)]^{+/0}$ and E_{pc} = −0.41 V for *trans*-$[Os^{VI}(tpy)(Cl)_2(N)]^{+/0}$ (0.1 M TBAH/CH_3CN, vs SSCE).[19] This observed reactivity is inconsistent with initial one-electron transfer and more consistent with the importance of initial electron donation from the nitrido complex to $SPPh_3$.

Acknowledgments are made to the National Science Foundation (Grant CHE-9503738) for support of this research.

Supporting Information Available: Listings of the X-ray experimental details, atomic coordinates, thermal parameters, and bond distances and angles for *cis*-$[Os^{IV}(tpy)(Cl)_2(NPPh_3)](PF_6)$. This material is available free of charge via the Internet at http://pubs.acs.org.

IC991425T

(18) Holt, E. M.; Holt, S. L. *Chem. Commun.* **1970**, 1704.
(19) Huynh, M. H. V.; El-Samanody, E.-S.; Demadis, K. D.; White, P. S.; Meyer, T. J. *Inorg. Chem.*, in press.
(20) Williams, D. S.; Coia, G. M.; Meyer, T. J. *Inorg. Chem.* **1995**, *34*, 586.
(21) The $E_{1/2}$ values are the averages of $E_{1/2}$ values for the sequential one-electron reductions of $[Os^{II}(tpy)(Cl)_2(NS)]^+$.